Desalination and Water Treatment
www.deswater.com

doi: 10.5004/dwt.2020.24880

174 (2020) 324–335
January

Removal of Cu(II), Co(II) and Pb(II) from synthetic and real wastewater using calcified *Solamen Vaillanti* snail shell

Hossein Esmaeili[a,*], Sajad Tamjidi[b], Mehrdad Abed[a]

[a]*Department of Chemical Engineering, Bushehr Branch, Islamic Azad University, Bushehr, Iran, emails: Esmaeili.hossein@gmail.com/ Esmaeili.hossein@iaubushehr.ac.ir (H. Esmaeili), mehrdad2665@yahoo.com (M. Abed)*
[b]*Young Researchers and Elite Club, Bushehr Branch, Islamic Azad University, Bushehr, Iran, email: tamjidisajad@gmail.com*

Received 14 March 2019; Accepted 9 September 2019

ABSTRACT

In this study, bioadsorbent powder of *Solamen Vaillanti* snail shell was used to remove lead, cobalt, and copper ions from synthetic and industrial wastewater. To do this, bioadsorbent powder was first prepared by the calcination of shellfish skin, and the physical properties of the bioadsorbent before and after the adsorption process were then studied using Brunauer–Emmett–Teller, scanning electron microscopy, Fourier-transform infrared spectroscopy, and energy dispersive X-ray analysis techniques. Also, the effect of different parameters such as pH, contact time, temperature, the initial concentration of metal ions, and adsorbent dosage on the removal efficiency of lead, cobalt and copper ions was investigated. The best adsorption efficiency was determined as pH 6 for cobalt and pH 5 for lead and copper, the temperature of 25°C, the contact time of 60 min, initial ion concentration 10 mg L^{-1}, and adsorbent dosage of 2 g L^{-1}. The maximum removal efficiencies of lead, cobalt, and copper ions were 94.4%, 96.5%, and 96.7%, respectively. Also, the maximum adsorption efficiency of lead, cobalt, and copper ions from industrial wastewater was obtained 85%, 81%, and 91%, respectively. The equilibrium behavior of the adsorption process indicated that the adsorption process follows the Langmuir isotherm model. Also, the pseudo-second-order kinetic model could better describe the kinetic behavior of the adsorption process. According to the Langmuir model, the highest adsorption capacity of lead, cobalt, and copper were obtained 26.04, 29.41 and 33.55 mg g^{-1}, respectively. The values of the thermodynamic parameters also showed that the adsorption process was feasible, spontaneous, and exothermic.

Keywords: Bioadsorbent; *Solamen Vaillanti*; Aqueous solution; Adsorption

1. Introduction

Over the past decades, due to the increasing growth of industrial operations, the introduction of contaminants such as heavy metals into the environment has significantly increased [1]. This leads to acute and chronic contamination of the biological population including plants, animals, and human beings [1,2]. These heavy metals are introduced into the natural ecosystem via natural soil erosion, volcanic eruptions, atmospheric precipitation, and wastewater discharge from various industries, including melting, plating, plastics, photography, tanning, producing, and consuming materials containing metals, and dye [3]. There are several types of metal ions in the environment such as arsenic, mercury, copper, iron, cobalt, lead, chromium, etc. which some of them are necessary for the human body. Among them, copper is one of the essential metals that is required in small amounts for the proper functioning of the human body [4]. In the human body, dietary intake of cobalt ion varies between 5–50 μg d^{-1} and it is an important component in vitamin B12 which is

* Corresponding author.

required for hemoglobin synthesis [5]. However, copper, cobalt, and lead are major pollutants of the environment in high concentrations [6,7]. The presence of these metals above the defined standards in the environment causes environmental problems and complications for living organisms as well as the environment. In fact, heavy metals are not eliminated from the body through natural excretion but are deposited and accumulated in tissues such as fat, muscle, bones and joints, leading to many diseases and complications such as [8] nausea, skin ulcers, lung cancer, disturbed function of liver and kidneys, and nerve disorders [7,8]. The permissible standard for existing lead and copper ions in drinking water is 0.01 and 0.05 mg L^{-1}, respectively [9]. Also, the permissible amount of cobalt in drinking water is 0.005 mg L^{-1} according to The World Health Organization (WHO) [10]. Therefore, their removal from wastewater and aqueous solutions is of great importance. There are several methods for the removal and separation of heavy metals from wastewater including, reverse osmosis, filtration, chemical oxidation, adsorption, deposition, electrochemical purification, chemical coagulation, and ion exchange [11–13]. The adsorption method is commonly used due to its high efficiency, simplicity, and low cost of adsorbents [6,7]. Among various adsorbents, bioadsorbents are one of the most promising materials for the removal of heavy metals from wastewater. The seashell skin is currently being used worldwide as a source of lime and nutrition for fish and livestock [14]. Several studies have been carried out on the removal of heavy metals using different adsorbents and bioadsorbents such as *Saccostrea cucullata* [14], nano-goethite and nano-hematite [15], bagasse and its ash [16], *Ziziphus spina-christi* leaf [17], *Phragmites australis*, baker's yeast, rice husk, *Aspergillus niger*, *Gracilaria caudata*, *Nostoc muscorum*, *Gloeocapsa gelatinosa*, and *Sargassum* sp. [18].

The main objective of this study was to use the calcined *Solamen Vaillanti* seashell (CSVS) as a bioadsorbent to remove heavy metal ions of copper, cobalt, and lead ions from synthetic and industrial wastewater prepared in phases 20 and 21 of the South Pars Gas Complex (SPGC) (Asaluyeh, Iran). To do this, the surface properties of the bioadsorbent as a new adsorbent were investigated using Brunauer–Emmett–Teller (BET), scanning electron microscopy (SEM), Fourier-transform infrared spectroscopy (FTIR), and energy dispersive X-ray analysis (EDX) analyses. Also, the effect of different parameters such as temperature, pH, contact time, metal ion concentration, and adsorbent dosage was studied. Moreover, kinetic, equilibrium and thermodynamic models were used to study the behavior of the adsorption process.

2. Materials and methods

2.1. Chemicals

To prepare stock solutions, $Pb(NO_3)_2$ (purity ≥ 99%), $CuSO_4 \cdot 5H_2O$ (purity ≥ 99%), NaOH (purity ≥ 97%), and HCl (37%) were purchased from Merck Company (Germany). Also, $Co(NO_3)_2$ (purity ≥ 98%) was purchased from Sigma-Aldrich Company (USA). To adjust the pH of the samples, the solutions of HCl (0.1 M) and NaOH (0.1 M) were used. Also, real wastewater was prepared from the SPGC in Phases 20 and 21 (Asaluyeh, Iran) and the amount of cobalt(II), lead(II) and copper(II) were measured. The wastewater contains small amounts of gas condensate and heavy metals in water.

2.2. Analytical methods

In this study, a flame atomic absorption spectrometry (GBC, Avanta) with acetylene-air fuel was used to determine the amount of copper, cobalt and lead in the solution. Also, Metrohm pH meter equipped with a glass electrode (Switzerland) was used to adjust the pH value of the solutions and an analytical balance digital scale with a precision of ±0.0001 was used to weigh up the materials. Moreover, the SEM analysis (Mira III, TESCAN, Czech Republic) was used to determine the morphology and to identify the structure of the materials before and after the adsorption process. Also, the elemental analysis or EDX (Mira III, TESCAN, Czech Republic) was applied to determine elemental compositions in the adsorbent. Furthermore, the FTIR analysis (Avatar, Thermo, USA) was used to specify the functional groups, and the BET analysis (Micromeritics, Asap 2020, USA) was used to estimate the specific surface area of the adsorbent. To determine the specific surface area of the adsorbent by BET analysis, 0.06 g of the sample was heated for 2 h at 120°C under nitrogen pressure.

2.3. Preparing bioadsorbent powder from Solamen Vaillanti

To prepare the bioadsorbent, the *Solamen Vaillanti* seashells were first collected, transferred to the laboratory, shattered, and then washed well with distilled water to remove dust and wastes. Afterward, they were placed in an oven for 30 min at a temperature of 100°C–110°C. In the next phase, 50 g of shells were mixed with a specific volume of phosphoric acid 95% with the volume ratio of 1:10, so that the surface of the shells was well impregnated with acid. The resulting mixture was transferred into the furnace and the temperature gradually reached 400°C within 2 h. The sample was then kept in the furnace at 400°C for 1 h until calcination was performed. The furnace was then turned off and slowly reached the ambient temperature. The produced powder was washed until its pH value reached 6.5. The final product was again placed in the oven for an hour at 120°C to be completely dried. Then, it was ground using a mortar and pestle and kept in a glass bottle to prevent moisture absorption.

2.4. Preparing stock solutions of cobalt, lead, and copper

In order to prepare the stock solutions of cobalt, lead, and copper with concentrations of 1,000 mg L^{-1}, 0.31, 0.25 and 0.16 g of $Co(NO_3)_2$, $CuSO_4 \cdot 5H_2O$ and $Pb(NO_3)_2$ were separately dissolved in 100 ml of double-distilled water, and it was then diluted with double distilled water to prepare solutions with different concentrations of metal ions.

2.5. Adsorption test

In this study, the effect of various parameters, including pH (2–10), contact time (10–80 min), temperature (25°C–55°C), initial concentration of heavy metal ions (10–50 mg L^{-1}), and adsorbent dosage (0.25–3.5 g L^{-1}) on the adsorption of lead(II), cobalt(II) and copper(II) from aqueous solution were examined. The experiments were performed with two replications and the results were presented as average values. The atomic absorption device was used to measure the number

of heavy metal ions remaining in the solution. In all samples, Eqs. (1) and (2) were used to determine the adsorption efficiency (% R) and adsorption capacity (q_e) of heavy metals, respectively:

$$\%R = \frac{(C_i - C_0)}{C_i} \times 100 \quad (1)$$

$$q_e = \frac{C_i - C_0}{M} \times V \quad (2)$$

where C_i and C_0 (mg L^{-1}) are the initial concentration and the equilibrium concentration of metal ions, respectively. Also, V, M, and q_e are the solution volume (L), the adsorbent weight (g), and the amount of ion adsorbed per gram of the adsorbent (mg g^{-1}), respectively [14].

3. Results and discussion

3.1. Characterization of the bioadsorbent

The BET analysis was performed using nitrogen gas on the CSVS. The results showed that the specific surface area, total pore volume, and mean pore diameter of the adsorbent prior to placement in the acid solution were 1.4 m^2 g^{-1}, 0.003 cm^3 g^{-1}, and 8.5 nm, respectively. Also, the specific surface area of the CSVS after placement in the acid solution was increased to 4.3815 m^2 g^{-1}. Also, the mean pore diameter of the adsorbent was achieved 15.94 nm which shows the CSVS is a mesoporous material. Therefore, the results showed that after activation by an acidic solution, the surface characteristics of the adsorbent has been improved. In previous studies, the specific surface area of some adsorbents such as golden apple snail shell [19], and calcined *Umbonium vestiarium* snail shell [20] were 2.1, and 17.02, respectively. Also, the specific surface area of calcined oyster shells at different temperatures of calcination was in the range of 1.8–64.6 [21]. Therefore, the results of previous studies were comparable with this study.

Furthermore, FTIR analysis was performed before and after the adsorption of metal ions to determine the functional groups on the adsorbent surface. This analysis also examined the strength of chemical bonds between atoms (covalent bonds) in molecular samples. Since the removal of heavy metals by the adsorbent (shellfish powder) was superficial and physical, no significant changes were observed in the FTIR spectrum of the CSVS before and after the adsorption process. Fig. 1 shows the FTIR spectrum of the CSVS before and after the adsorption process. As shown in the FTIR spectrum of the adsorbent before the adsorption process, the peak at 3,443 cm^{-1} is related to the hydroxyl group (OH), which can be due to the presence of this group in its structure or the adsorption of moisture. The shells are calcareous ($CaCO_3$), so the peaks at 859; 1,079; and 1,475 cm^{-1} belong to the vibrating groups (flexural vibration, asymmetric and symmetric tensile vibration) of the carbonate group (O–C–O). Further, the peak at 1,790 cm^{-1} belongs to the C=O bond of the carbonate group [6,22]. The peak at 705 cm^{-1} might also belong to the Mn–O group [23].

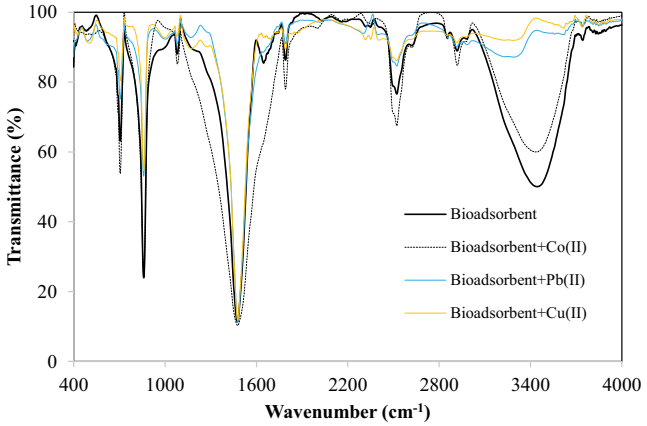

Fig. 1. FTIR spectra of bioadsorbent before and after adsorption of Co(II), Pb(II), and Co(II).

Also, SEM analysis was used to assess the surface morphology of the adsorbent before and after adsorption of cobalt, lead and copper ions. Fig. 2a shows the surface of the adsorbent before the adsorption process. Also, Figs. 2b–d indicate the adsorbent surface after the adsorption of cobalt, lead, and copper ions. As can be observed in Fig. 2, the adsorption surface significantly changed and became rougher, which may be due to the adsorption of metal ions on the active sites of the CSVS.

In the EDX analysis, the constituents of the sample in a semi-quantitative form can be detected. Fig. 3 shows an elemental analysis of the CSVS before and after the removal of lead(II), cobalt(II) and copper(II) ions. Also, the results of Fig. 3 are given in Table 1. As shown, there are Ca, Mn, O, and Si elements on the adsorbent surface before the adsorption process (Fig. 3a), and metal ions such as lead(II), cobalt(II) and copper(II) are not observed. After adsorption of Co(II), Pb(II), and Cu(II), the results are shown in Figs. 3b–d. Also, the weight and atomic percentage of the elements are presented in Table 1. As seen in Table 1, these heavy metals are adsorbed by the adsorbent and the weight percent of Co(II), Pb(II), and Cu(II) were 0.49%, 0.63%, and 1.1%, respectively which shows the presence of these heavy metals on the adsorbent surface after adsorption process.

Also, the removal mechanism of heavy metals by the CSVS is shown in Fig. 4. The CSVS contains Ca, C, and O elements which adsorb heavy metal ions of Pb(II), Co(II), and Cu(II) which are displayed in Fig. 4.

3.2. Impacts of different parameters on the adsorption process

3.2.1. Effect of pH

The initial pH of the solution affects the changes in surface charge of the adsorbent and the ionization degree of the adsorbed ions in the adsorption process. Also, the adsorption mechanism is highly dependent on this parameter [22,24]. The effect of pH on the adsorption of copper, cobalt, and lead by *Solamen Vaillanti* adsorbent is shown in Fig. 5 at various pH values ranging from 2 to 10 while the other parameters were kept constant (contact time of 70 min, the temperature of 25°C, initial metal ion concentration of

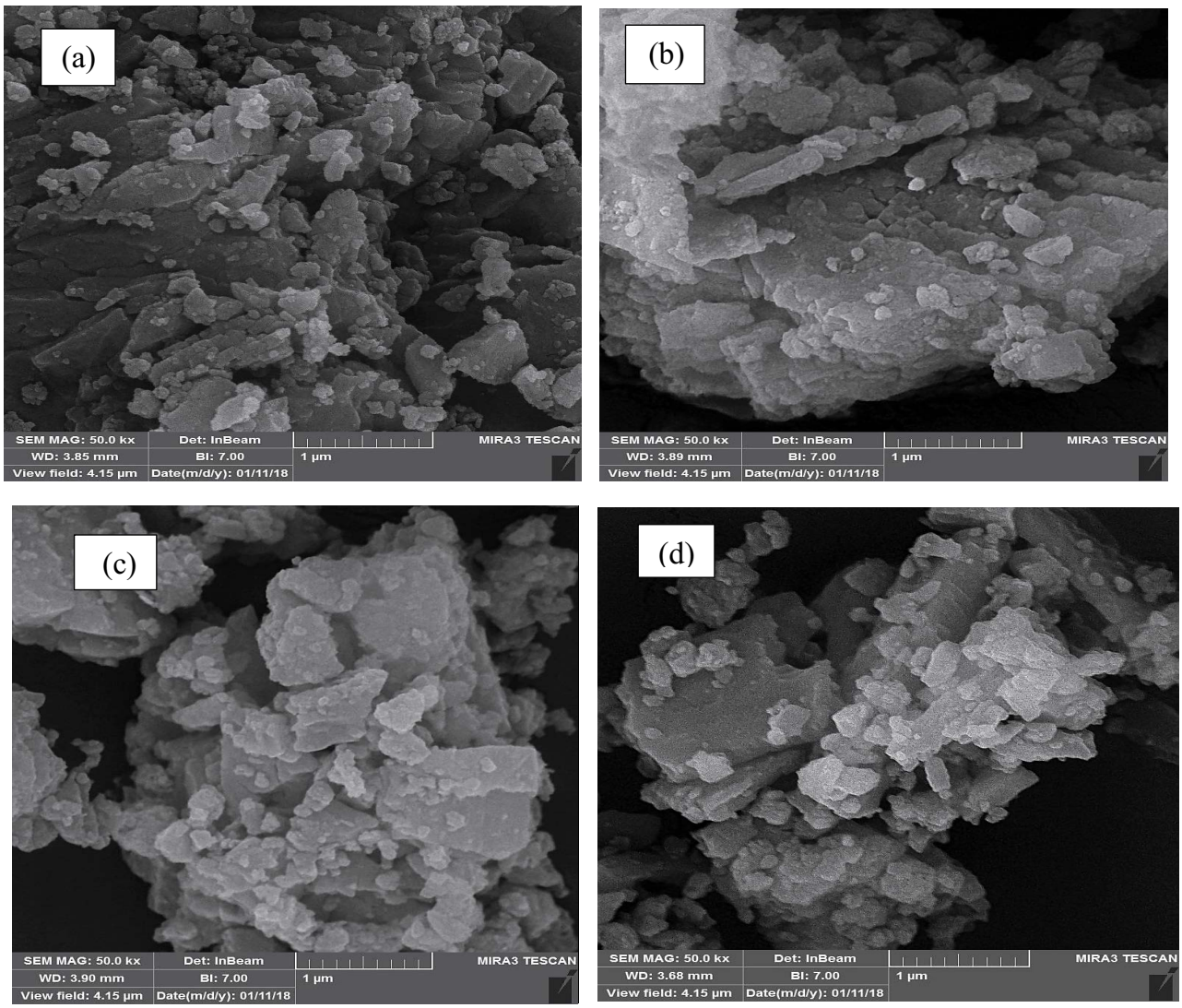

Fig. 2. SEM images of (a) bioadsorbent, (b) bioadsorbent with Co(II) ions, (c) bioadsorbent with Pb(II) ions, and (d) bioadsorbent with Cu(II) ions.

10 mg L^{-1}, the adsorbent dosage of 0.25 g L^{-1}, and mixing the speed of 200 rpm). At low pH values, there is a competition between hydrogen ions (H^+) in the solution and metal ions to sit on the active sites of the bioadsorbent. Hydrogen ions (H^+) prevent metal ions from sitting on adsorbent sites so that a repulsive force is formed between the hydrogen ions (H^+) and heavy metal ions, which reduces the removal efficiency [20]. When the pH of the solution increases, the number of hydrogen ions (H^+) in the aqueous solution is decreased. As a result, more active sites are available for the placement of copper, cobalt, and lead, and this increases the electrostatic gravity between copper, cobalt, and lead ions with the adsorbent active sites and thus increase the adsorption efficiency. At pH > 6, due to the deposition of metal ion hydroxide, the adsorption efficiency decreased [25]. Therefore, the adsorption efficiency of 86.2% and 81.5% were considered as optimal values for lead and copper at the pH value of 5 and adsorption efficiency of 80.5% was optimal for cobalt ions at the pH value of 6.

3.2.2. *Effect of lead, cobalt and copper ion concentration*

Fig. 6 presents the effect of the initial concentration of lead, cobalt and copper ions (10, 20, 30 and 50 mg L^{-1}) on the adsorption efficiency under optimal pH for lead and copper (pH = 5) and cobalt (pH = 6), contact time of 70 min, temperature of 25°C, adsorbent dosage of 0.25 g L^{-1}, and mixing speed of 200 rpm. As can be observed, with increasing concentration from 10 to 50 mg L^{-1}, the removal efficiency of lead, cobalt, and copper was decreased, so that the initial concentration of 10 mg L^{-1} for lead, cobalt, and copper with the removal efficiency of 86.2%, 80.5%, and 81.5% was considered as optimal concentration, respectively. At low concentrations of heavy metal ions in the solution, due to the presence of sufficient active sites and easier access, the adsorption process is facilitated and the adsorption efficiency rises. At high concentrations, due to the presence of more heavy metal ions in the solution and less access to active sites since they are saturated, the removal efficiency decreases [6,26].

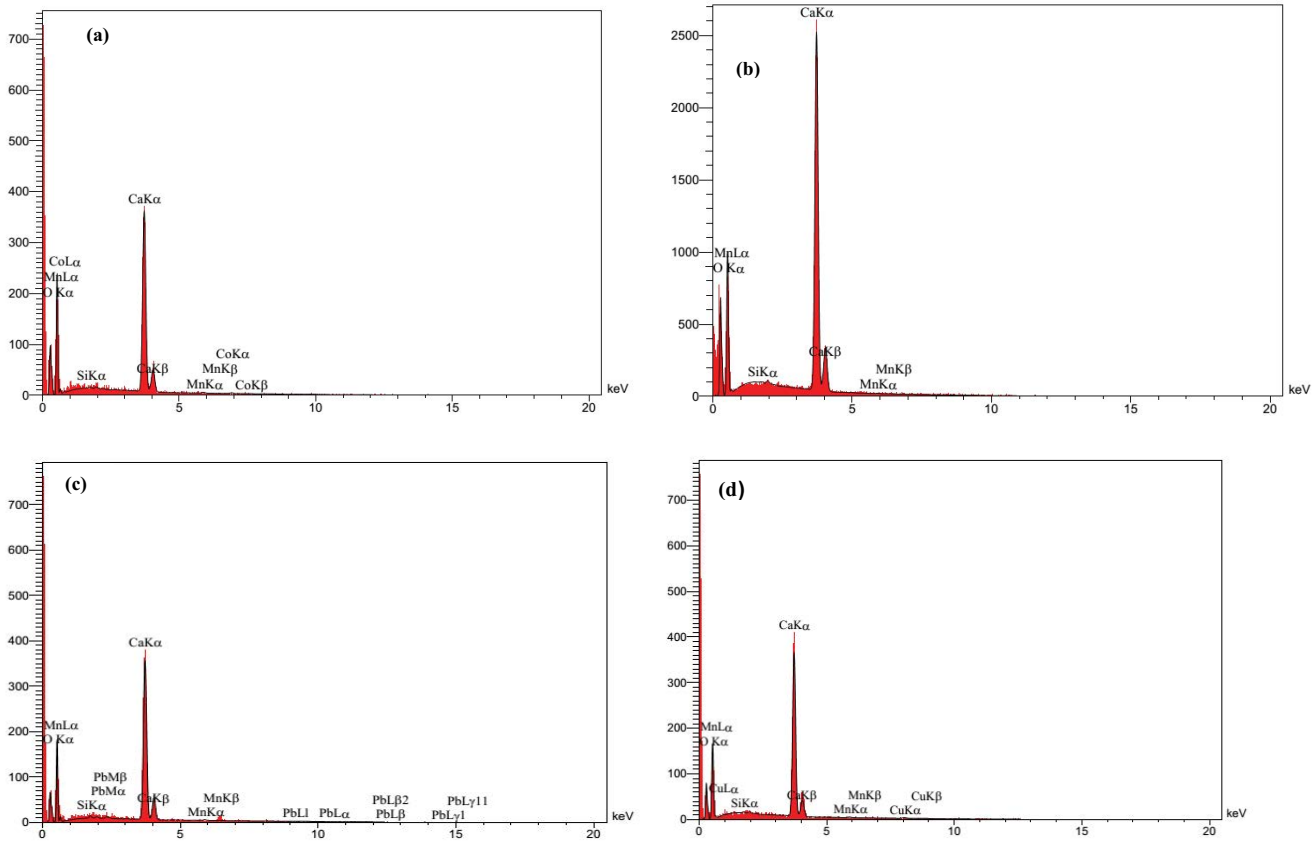

Fig. 3. EDX analysis of (a) adsorbent, (b) adsorbent with Co(II) ions, (c) adsorbent with Pb(II) ions, and (d) adsorbent with Cu(II) ions

Table 1
Elements percentage in the CSVS before and after adsorption of Co(II), Pb(II), and Cu(II)

Element	Bioadsorbent		Bioadsorbent after adsorption of Co(II)		Bioadsorbent after adsorption of Pb(II)		Bioadsorbent after adsorption of Cu(II)	
	Wt.%[a]	At.%[b]	Wt.%	At.%	Wt.%	At.%	Wt.%	At.%
C	18.17	28.22	17.79	27.24	14.98	24.07	15.38	24.24
O	48.09	56.08	50.89	58.50	48.60	58.64	50.72	59.99
Si	–	–	0.07	0.04	0.19	0.13	0.05	0.03
Ca	33.67	15.67	30.41	13.95	35.19	16.95	32.37	15.28
Mn	0.07	0.03	0.35	0.12	0.41	0.14	0.37	0.13
Co(II)	–	–	0.49	0.15	–	–	–	–
Pb(II)	–	–	–	–	0.63	0.06	–	–
Cu(II)	–	–	–	–	–	–	1.10	0.33
Total	100	100	100	100	100	100	100	100

[a]Weight percent.
[b]Atomic percent.

3.2.3. Effect of contact time

Fig. 7 shows the effect of contact time (10, 15, 20, 30, 35, 40, 45, 50, 60, 70 and 80 min) on the adsorption efficiency of lead, cobalt, and copper under optimal pH conditions for copper and lead (pH = 5) and, cobalt (pH = 6), the temperature of 25°C, the initial metal ion concentration of 10 mg L^{-1}, the adsorbent dosage of 0.25 g L^{-1}, and mixing rate of 200 rpm. The results showed that the adsorption process at different temperatures encompasses two stages: the initial stage (shorter period) and the second stage (longer period). According to Fig. 7, due to a large number of unsaturated active sites in the early phase, the adsorption of metal ions increased rapidly as the contact

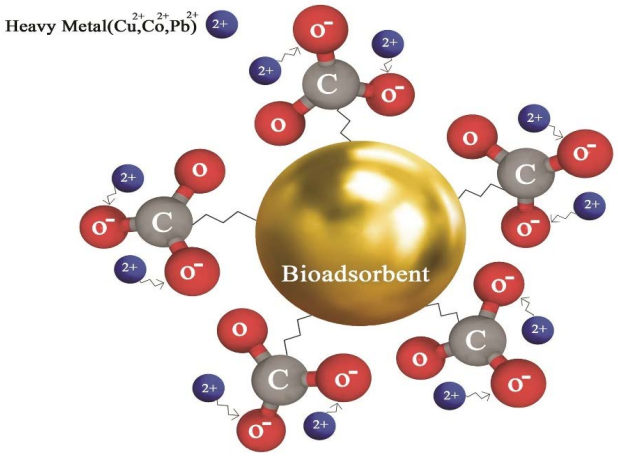

Fig. 4. Proposed mechanism for removal of Cu(II), Co(II) and Pb(II) using the CSVS.

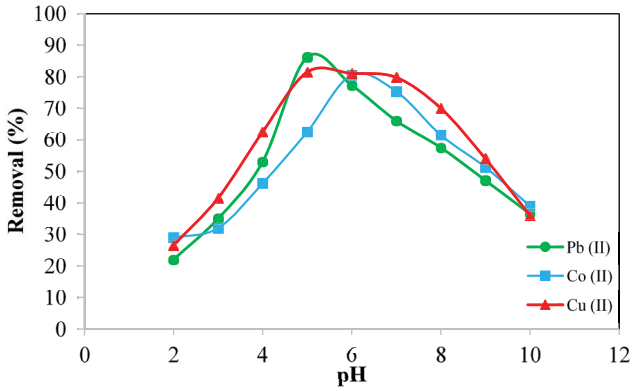

Fig. 5. Effect of pH on the removal of copper, cobalt and lead from aqueous media using the CSVS (temperature: 25°C, contact time: 70 min, adsorbent dose: 0.25 g L^{-1}, C_i: 10 mg L^{-1}, mixture rate: 200 rpm).

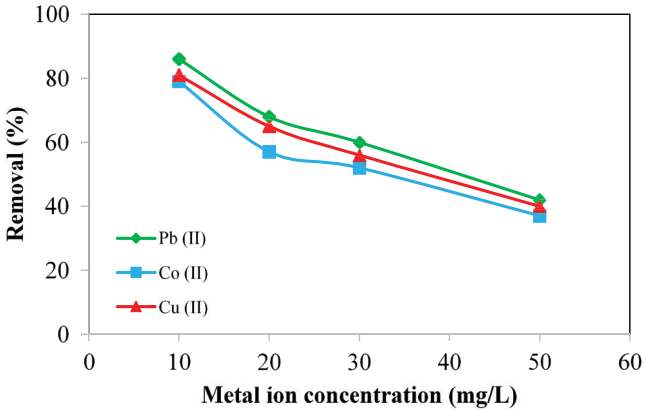

Fig. 6. Effect of initial metal ion concentration on the removal of copper, cobalt and lead from aqueous media using the CSVS (pH for copper and lead: 5, pH for cobalt: 6, temperature: 25°C, contact time: 70 min, adsorbent dose: 0.25 g L^{-1}, mixture rate: 200 rpm).

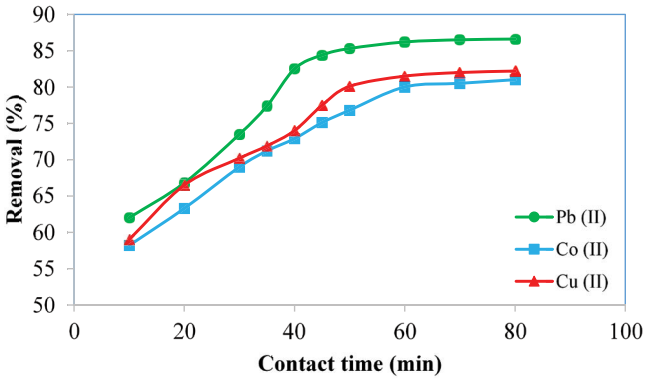

Fig. 7. Effect of time on the removal of copper, cobalt and lead from aqueous media using the CSVS (pH for Copper and lead: 5, pH for cobalt: 6, adsorbent dose: 0.25 g L^{-1}, C_i: 10 mg L^{-1}, mixture rate: 200 rpm).

time increased. With increasing contact time after 60 min, no increase in the removal percentage was observed. In the next phase, due to the gradual saturation of active sites, the adsorption rate slowly decreased because of a decrease in active sites of the adsorbent and intra-particle penetration process. After transferring ions to the adsorbent surface, the intra-particle penetration occurred in the second stage, and this slow process is caused by penetrating metal ions into the adsorbent surface [6,14,27].

3.2.4. Effect of bioadsorbent dosage

Adsorption dosage is one of the most significant parameters in the adsorption process since it determines the maximum adsorption capacity in removing pollutants [28]. The effect of adsorbent dosage (0.25–3.5 g L^{-1}) on the adsorption efficiency of lead, cobalt, and copper ions from aqueous solution using the CSVS is shown in Fig. 8. According to the results, it was found that the adsorption efficiency decreased in low adsorbent dosages due to the lack of sufficient active sites to sit lead, cobalt and copper on the adsorbent surface. In high adsorbent dosages, the density of active sites on the adsorbent surface is enhanced so that the removal efficiency is increased. Then the slope of the graph is constant and linear regarding the saturation of active sites on the adsorbent surface [24–28]. Thus, with an increase in the adsorbent dosage from 0.25 to 2.5 g L^{-1}, the adsorption efficiency increased and no significant changes were observed in the adsorption efficiency for an adsorbent dose greater than 2.5 g L^{-1}. Consequently, the concentration of 2.5 g L^{-1} was considered as the optimum value with the adsorption efficiencies of 94.4%, 96.5%, and 96.7% for lead, cobalt and copper ions, respectively.

3.2.5. Effect of temperature

Fig. 9 shows the effect of temperature on the adsorption of lead, cobalt, and copper using the CSVS. As seen in the figure, the removal efficiency enhanced by increasing temperature from 15°C to 25°C and the highest removal percentages were obtained 94.4%, 96.5% and 96.7% for lead, cobalt,

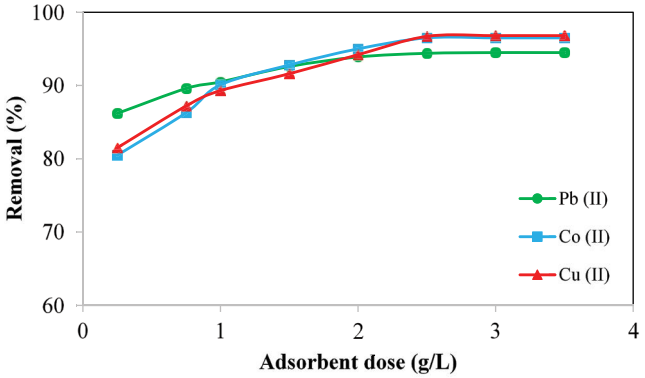

Fig. 8. Effect of adsorbent dosage on the removal of copper, cobalt and lead from aqueous media using the CSVS (pH for copper and lead: 5, pH for cobalt: 6, temperature: 25°C, contact time: 60 min, C_i: 10 mg L^{-1}, mixture rate: 200 rpm).

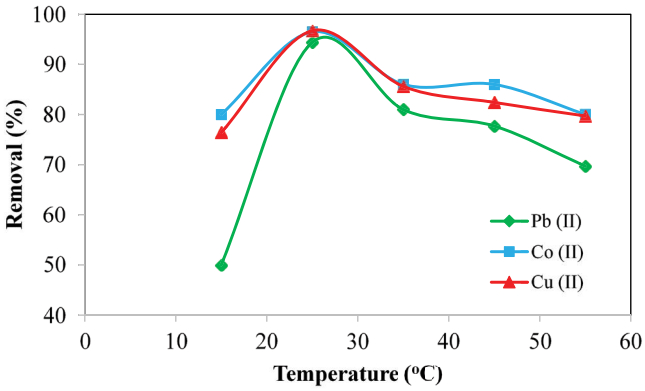

Fig. 9. Effect of temperature on the removal of copper, cobalt and lead from aqueous media using the CSVS (pH for copper and lead: 5, pH for cobalt: 6, adsorbent dose: 2.5 g L^{-1}, contact time: 60 min, C_i: 10 mg L^{-1}, mixture rate 200 rpm).

and copper, respectively. At temperatures greater than 25°C, the removal efficiency of heavy metal ions reduced, indicating that the adsorption process was exothermic [6,14,27]. The increasing tendency of the ions toward separation from the surface of the adsorbent, inactivating some of the active sites, and weakening of the attraction force between the ions and active sites of the adsorbent can be referred to as causes of reduced removal efficiency by increasing solution temperature [24]. Therefore, 25°C was considered as the optimum temperature.

3.2.6. Study of adsorption isotherms

To study the isothermal behaviors of lead, cobalt and copper ion adsorption, Langmuir and Freundlich isotherm models were used. The Langmuir isotherm model is defined based on the uniform (homogeneous) adsorption of the adsorbed with the same energy on all adsorbent surfaces. The linear form of the Langmuir isotherm model is given in Eq. (3).

$$\frac{C_e}{q_e} = \frac{1}{K_L q_m} + \frac{1}{q_m} C_e \tag{3}$$

where q_e is the adsorbed component per gram of adsorbent in mg g^{-1}, C_e is the concentration of the adsorbed in the solution after the adsorption process in mg L^{-1}, q_m is the maximum adsorption capacity in mg g^{-1}, and K_L is the isotherm constant. Withdrawing the C_e/q_e curve in terms of C_e, the gradient and y-intercept of the graph can be calculated [29,30].

Freundlich isotherm model is defined based on the multi-layer adsorption on heterogeneous surfaces and non-uniform distribution of energy on the active sites of the adsorbent. The linear form of the Freundlich isotherm model is expressed as follows.

$$\ln\left(q_e\right) = \ln K_f + \frac{1}{n} \ln C_e \tag{4}$$

where C_e is the equilibrium concentration (mg L^{-1}), q_e is the adsorption capacity at equilibrium time (mg L^{-1}), and K_f and n are also the Freundlich model constants [30,31]. Fig. 10 shows the Langmuir and Freundlich isotherm plots of the adsorption process of lead, cobalt, and copper using the CSVS.

The results suggested that the Langmuir isotherm model could better describe the equilibrium behavior of the adsorption process than the Freundlich isotherm model, thus homogeneous surfaces had a greater contribution to the metal ion adsorption. The maximum adsorption capacity of the adsorbent using the Langmuir isotherm model was 26.04, 29.41, and 33.55 mg g^{-1} for lead, cobalt, and copper, respectively. Also, the correlation coefficients (R^2) for the adsorption process of lead, cobalt, and copper ions were obtained 0.9975, 0.997, and 0.999 based on Langmuir isotherm model, suggesting that the experimental data were fitted well with the Langmuir model. The maximum adsorption capacity as compared to previous studies and the results is presented in Table 2. As shown in this Table, the maximum adsorption capacity in this study is comparable to previous studies.

3.2.7. Kinetic study

To investigate the kinetic behavior of adsorption of lead, cobalt, and copper, pseudo-first-order, pseudo-second-order, and intraparticle diffusion kinetic models were used. The linear form of the pseudo-first-order kinetic model or Lagrangian model is expressed as follows:

$$\ln\left(q_e - q_t\right) = \ln\left(q_e\right) - k_1 t \tag{5}$$

where q_e is the adsorbed ion in the equilibrium state per gram of the adsorbent (mg g^{-1}), q_t is the adsorbed ion per gram of the adsorbent at time t (mg g^{-1}), and k_1 is the constant rate of adsorption in the pseudo-first-order kinetic model (min^{-1}) [42,43]. The linear form of the pseudo-first-order kinetic model is plotted in Fig. 11.

The linear form of the pseudo-second-order kinetic model is also given by Eq. (6).

$$\frac{t}{q_t} = \frac{1}{k_2 q_e^2} + \frac{t}{q_e} \tag{6}$$

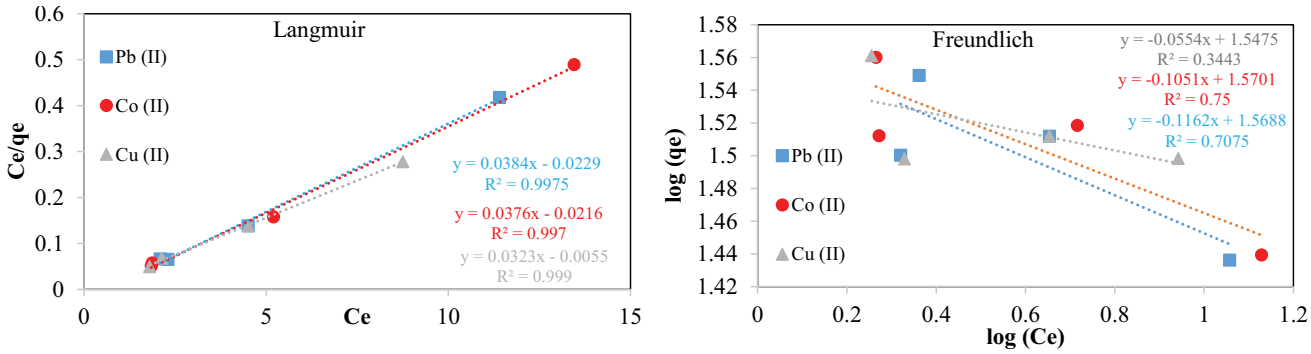

Fig. 10. Langmuir and Freundlich linear isotherm plots related to the adsorption of Pb(II), Co(II) and Cu(II) ions using the CSVS (pH for copper and lead: 5, pH for cobalt: 6 adsorbent dose: 2.5 g L^{-1}, contact time: 60 min, temperature: 25°C, mixture rate: 200 rpm).

Table 2
Comparison of maximum adsorption capacity between the CSVS and other bioadsorbents for the removal of lead, cobalt and copper ions

Metal ions	Bioadsorbent	q_{max} (mg g^{-1})	References
Lead	Carbon gel	16.95	[32]
	Perlite	6.27	[33]
	Sargassum vulgare	9.9	[34]
	Agaricus campestris	5.8	[34]
	Layered-double-hydroxides-coated/hollow carbon microsphere composites	205.68	[35]
	Molybdenum disulfide/reduced graphene oxide	384.16	[36]
	Fe3O4/polydopamine nanoparticles	57.25	[37]
	Solamen Vaillanti	26.04	Present work
Cobalt	Carbon gel	5.46	[32]
	Perlite	1.05	[33]
	Kaolinite	0.919	[38]
	Padina sanctae-crucis	13.73	[39]
	Graphene oxide	43.6	[40]
	Magnetic graphene oxide (MGO)	23.2	[40]
	N-doped graphene oxide	27.3	[40]
	N-doped MGO	14.6	[40]
	Solamen Vaillanti	29.41	Present work
Copper	Carbon gel	6.64	[32]
	Fe3O4/polydopamine nanoparticles	86.35	[37]
	Kaolinite	10.78	[38]
	Padina sanctae-crucis	13.99	[39]
	Pomegranate peel	30.12	[41]
	Solamen Vaillanti	33.55	Present work

where k_2 is the constant rate of adsorption in the pseudo-second-order kinetic model (mg g^{-1} min^{-1}) [42,43]. Fig. 12 shows the equilibrium graph of the pseudo-second-order kinetic model in the adsorption process.

Also, the linear form of the intraparticle diffusion model is presented as follows [44]:

$$q_t = K_i t^{0.5} + I \quad (7)$$

where K_i and I are the intraparticle diffusion rate constant (mg g^{-1} $min^{-0.5}$) and boundary layer thickness which is determined from the slope and intercept of q_t against $t^{0.5}$ according to Fig. 13.

The correlation coefficients obtained from the pseudo-first-order, pseudo-second-order and intraparticle diffusion kinetic models in the concentrations of 10, 20 and 50 revealed that the pseudo-second-order kinetic model could better describe the kinetic behavior of the adsorption process. According to the results obtained from the intraparticle diffusion model, it can be said that the mechanism of adsorption has one step which has a high slope, in which the molecules of heavy metal ions are transferred directly

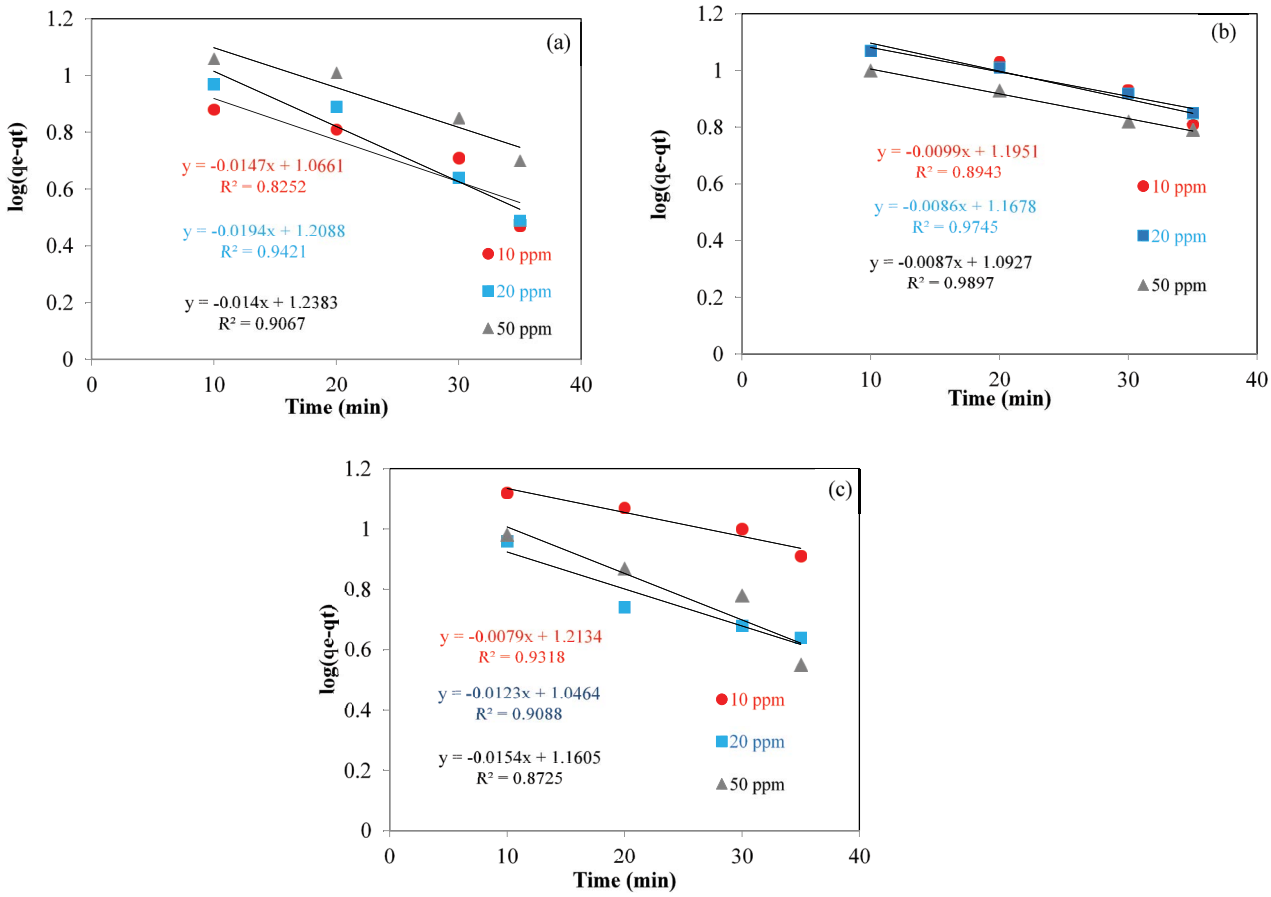

Fig. 11. Pseudo-first-kinetic model plots related to the adsorption of (a) Pb(II), (b) Co(II), and (c) Cu(II) ions (pH for copper and lead: 5, pH for cobalt: 6, adsorbent dose: 2.5 g L^{-1}, temperature: 25°C, mixture rate: 200 rpm).

from the layer to the adsorbent surface, and is carried out at a high speed.

3.2.8. Thermodynamic study

The thermodynamic parameters include changes in enthalpy ($\Delta H°$), entropy ($\Delta S°$) and Gibbs free energy ($\Delta G°$). Eq. (8) is used to calculate $\Delta G°$:

$$\Delta G° = -RT \ln K_c \tag{8}$$

where R is the universal gas constant (8.314 J mol^{-1} K^{-1}), T is the absolute temperature (K) and K_c is the equilibrium constant obtained from Eq. (9).

$$K_c = \frac{C_{ad,eq}}{C_{eq}} \tag{9}$$

where $C_{ad,eq}$, and C_{eq} are the concentration of metal ion adsorbed on the adsorbent surface at equilibrium state (mg L^{-1}) and the concentration of metal ion remaining in solution at equilibrium state (mg L^{-1}), respectively. $\Delta H°$ and $\Delta S°$ can be calculated from the slope and intercept of $\ln K_c$ against $1/T$ according to Eq. (10) [44,45].

$$\ln K_c = \frac{-\Delta G°}{RT} = \frac{-\Delta H°}{RT} + \frac{\Delta S°}{R} \tag{10}$$

Fig. 14 shows the thermodynamic parameters of heavy metals adsorption from wastewater using the CSVS. The thermodynamic parameters obtained from Fig. 14 are reported in Table 3.

Regarding the parameters shown in Table 3, the amount of Gibbs free energy was negative at all temperatures, indicating that the adsorption process of Pb(II), Co(II), and Cu(II) using the adsorbent was spontaneous and feasible. Also, the enthalpy change was negative showed that the adsorption process was exothermic. Also, the negative value of entropy for metal ions reflects a decrease in the bioadsorbent heterogeneity compared to the early phase before the adsorption process and reduces the degree of freedom at the solid–liquid common surface during the adsorption process [46].

3.2.9. Evaluating the adsorption efficiency for metal ions from real wastewater

To further investigate the adsorption process of Pb(II), Co(II) and Cu(II) ions using the CSVS, a sample of industrial wastewater was prepared from SPGC (Phases 20 and 21) and the amounts of cobalt(II), lead(II) and copper(II) ions were

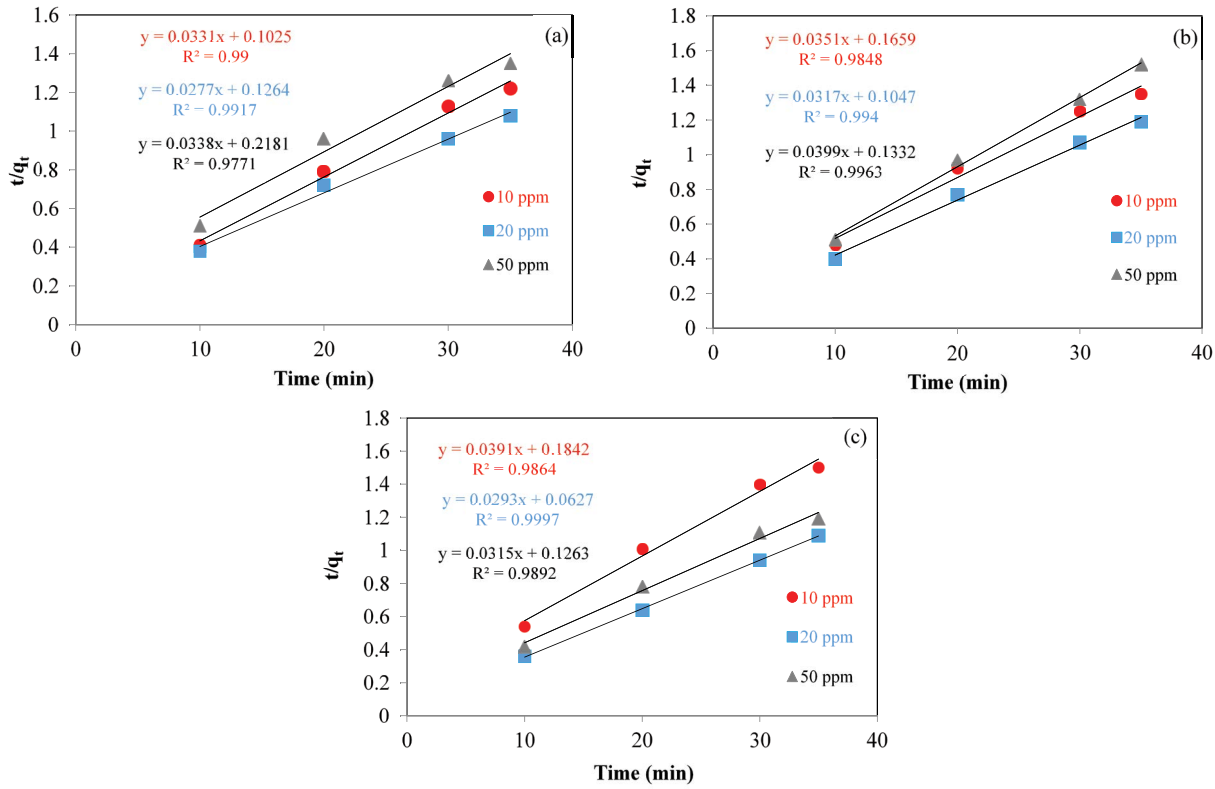

Fig. 12. Pseudo-second-kinetic model plots related to the adsorption of (a) Pb(II), (b) Co(II), and (c) Cu(II) ions (pH for copper and lead: 5, pH for cobalt: 6, adsorbent dose: 2.5 g L^{-1}, temperature: 25°C, mixture rate: 200 rpm).

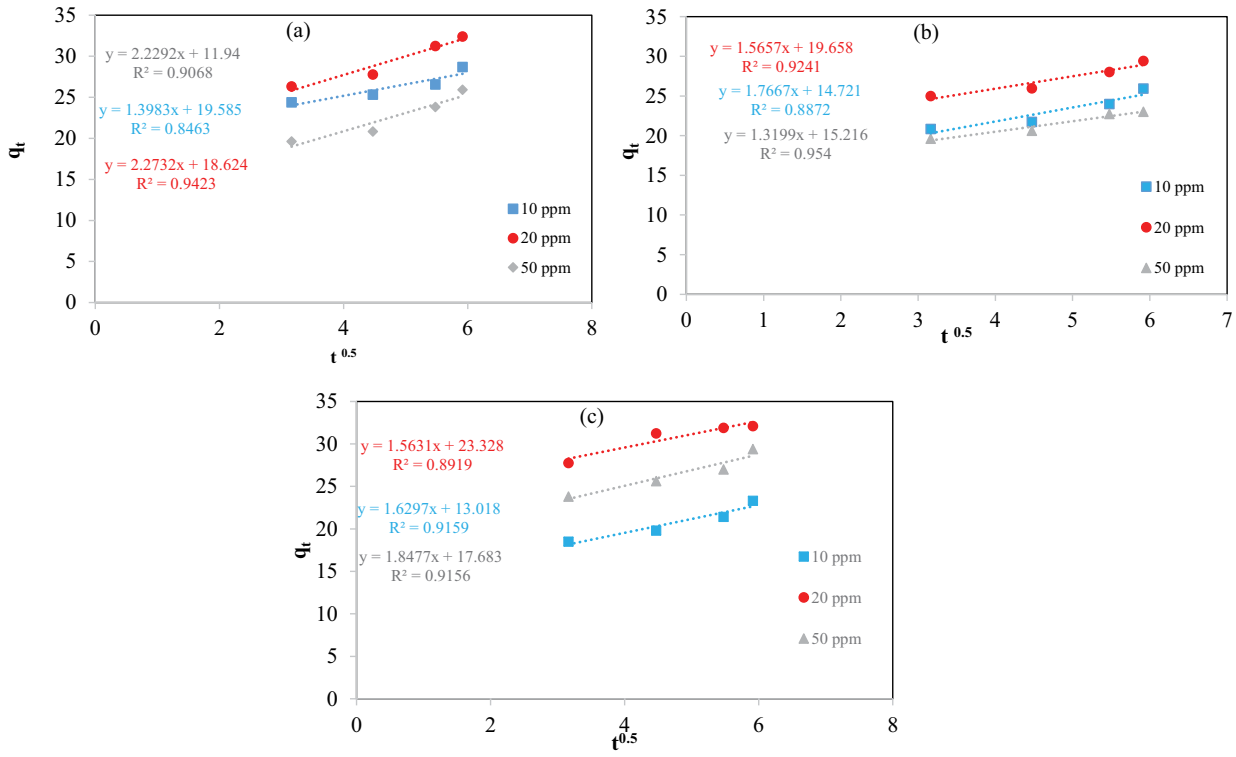

Fig. 13. Intraparticle diffusion kinetic model plots related to the adsorption of (a) Pb(II), (b) Co(II), and (c) Cu(II) ions (pH for copper and lead: 5, pH for cobalt: 6, adsorbent dose: 2.5 g L^{-1}, temperature: 25°C, mixture rate: 200 rpm).

Table 3
Thermodynamic parameters for the adsorption of Pb(II), Co(II), and Cu(II) onto the CSVS

Ions	$\Delta H°$ (kJ mol^{-1})	$\Delta S°$ (J mol^{-1} K^{-1})	$\Delta G°$ (kJ mol^{-1})			
			288.15 K	298.15 K	308.15 K	328.15 K
Cobalt	–48.13	–134.13	–9.50	–8.19	–6.80	–4.17
Lead	–51.54	–149.23	–8.60	–7.14	–5.65	–2.67
Copper	–53.37	–150.17	–10.17	–8.67	–7.17	–4.78

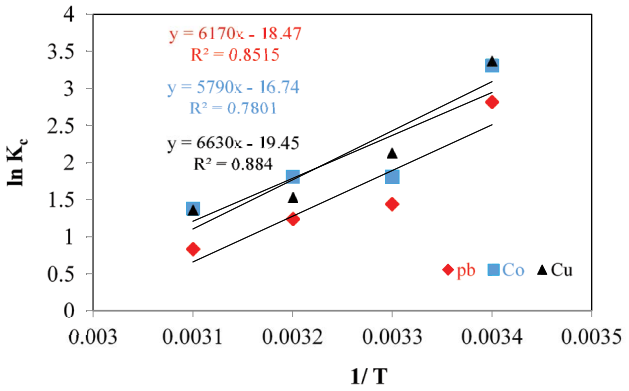

Fig. 14. Plot of lnK_c against T^{-1} for the determination of thermodynamic parameters for the adsorption of Pb(II), Co(II) and Cu(II) using the CSVS (pH for copper and lead: 5, pH for cobalt: 6, adsorbent dose: 2.5 g L^{-1}, mixture rate: 200 rpm).

Table 4
Removal of copper, cobalt, and lead by the CSVS from real wastewater

Ions	Add (ng ml^{-1})	Found (ng ml^{-1})	Removal (%)
Cobalt	0	0	–
	5	5.2	74
	15	15.3	81
Lead	0	0	–
	10	10.4	76
	20	20.2	85
Copper	0	2	88
	10	10.2	83
	20	19.4	91

measured. Table 4 shows the results of the adsorption process from industrial wastewater under optimal pH for lead, copper (pH = 5) and cobalt (pH = 6), contact time of 60 min, the temperature of 25°C, the adsorbent dosage of 2 g L^{-1}, and mixing speed of 200 rpm. Accordingly, it was found that the maximum adsorption efficiency for lead, cobalt, and copper was obtained as 85%, 81%, and 91%, respectively, indicating the optimal efficiency of the concerned adsorbent in the removal of metal ions from real wastewater.

4. Conclusion

In this study, the bioadsorbent powder of the CSVS was used to eliminate lead, cobalt and copper ions from synthetic and industrial wastewater in Phases 20 and 21 of the SPGC (Iran). To this end, the effect of different parameters such as pH, contact time, temperature, the initial concentration of metal ions, and adsorption dosage was examined. The results showed that the best removal efficiency of lead, cobalt, and copper was obtained as 94.4, 96.5 and 96.7, respectively which are obtained under conditions of pH 6 for cobalt and pH 5 for lead and copper, temperature of 25°C, contact time of 60 min, metal ion concentration of 10 mg L^{-1}, and adsorbent concentration of 2 g L^{-1}. Also, the maximum removal efficiency from industrial wastewater was obtained 85%, 81%, and 91% for lead, cobalt, and copper, respectively. High adsorption efficiency along with low cost confirms the desirable potential of the CSVS in removing metal ions from real and synthetic wastewater. After determining the optimum conditions, Langmuir and Freundlich isotherm models were used to determine the equilibrium behavior of metal ions adsorption. With greater correlation coefficients, the Langmuir isotherm model had better consistency with the experimental data than the Freundlich isotherm model. To study the kinetic behavior of the adsorption process, pseudo-first-order, pseudo-second-order, and intraparticle diffusion kinetic models were used and the result revealed that the pseudo-second-order kinetic model could better describe the kinetic behavior of the adsorption process. Also, the values of the thermodynamic parameters suggested that the adsorption process of lead, cobalt, and copper from wastewater using the aforementioned bioadsorbent was appropriate, spontaneous, and exothermic.

References

[1] C. Cojocaru, G. Zakrzewska-Trznadel, A. Jaworska, Removal of cobalt ions from aqueous solutions by polymer assisted ultrafiltration using experimental design approach. Part 1: optimization of complexation conditions, J. Hazard. Mater., 169 (2009) 599–609.
[2] A. Khan, J.L. Xing, A.M. Elseman, P.C. Gu, K. Gul, Y.J. Ai, R. Jehan, A. Alsaedi, T. Hayat, X.K. Wang, A novel magnetite nanorod-decorated Si-Schiff base complex for efficient immobilization of U(VI) and Pb(II) from water solutions, Dalton Trans., 47 (2018) 11327–11336.
[3] A. Sarı, M. Tuzen, Biosorption of cadmium(II) from aqueous solution by red algae (*Ceramium virgatum*): equilibrium, kinetic and thermodynamic studies, J. Hazard. Mater., 157 (2008) 448–454.
[4] W. Forth, Introduction to the Afternoon Session on Physiological Aspectes of Copper Metabolism, In: Inflammatory Diseases and Copper, Humana Press, 1982, pp. 73–74.
[5] A. Davenport, Trace Elements in Patients with Chronic Kidney Disease, In: Chronic Renal Disease, Academic Press, 2015, pp. 429–439.
[6] F. Ahmadi, H. Esmaeili, Chemically modified bentonite/Fe_3O_4 nanocomposite for Pb(II), Cd(II), and Ni(II) removal from synthetic wastewater, Desal. Wat. Treat., 110 (2018) 154–167.

[7] F.L. Fu, Q. Wang, Removal of heavy metal ions from wastewaters: a review, J. Environ. Manage., 92 (2011) 407–418.
[8] A. Ahmadpour, M. Tahmasbi, T.R. Bastami, J.A. Besharati, Rapid removal of cobalt ion from aqueous solutions by almond green hull, J. Hazard. Mater., 166 (2009) 925–930.
[9] J. Hussain, I. Husain, M. Arif, N. Gupta, Studies on heavy metal contamination in Godavari river basin, Appl. Water Sci., 7 (2017) 4539–4548.
[10] E.T. Gyamfi, M. Ackah, A.K. Anim, J.K. Hanson, L. Kpattah, S. Enti-Brown, Y. Adjei-Kyereme, E.S. Nyarko, Chemical analysis of potable water samples from selected suburbs of Accra, Ghana, Int. Acad. Ecol. Environ. Sci., 2 (2012) 118–127.
[11] X. Xu, B.Y. Gao, Q.Y. Yue, Q. Li, Y. Wang, Nitrate adsorption by multiple biomaterial based resins: application of pilot-scale and lab-scale products, Chem. Eng. J., 234 (2013) 397–405.
[12] Y.H. Wu, H.W. Pang, Y. Liu, X.X. Wang, S.J. Yu, D. Fu, J.R. Chen, X.K. Wang, Environmental remediation of heavy metal ions by novel-nanomaterials: a review, Environ. Pollut., 246 (2019) 608–620.
[13] Q. Huang, S. Song, Z. Chen, B.W. Hu, J.R. Chen, X.K. Wang, Biochar-based materials and their applications in removal of organic contaminants from wastewater: state-of-the-art review, Biochar, 1 (2019) 45–73.
[14] B. Heidari, A. Riyahi Bakhtiari, G. Shirneshan, Concentrations of Cd, Cu, Pb and Zn in soft tissue of oyster (*Saccostrea cucullata*) collected from the Lengeh Port coast, Persian Gulf, Iran: a comparison with the permissible limits for public health, Food Chem., 141 (2013) 3014–3019.
[15] Y.-H. Chen, F.-A. Li, Kinetic study on removal of copper(II) using goethite and hematite nano-photocatalysts, J. Colloid Interface Sci., 347 (2010) 277–281.
[16] K.Y. Ho, G. Mckay, K.L. Yeung, Selective adsorbents from ordered mesoporous silica, Langmuir, 19 (2003) 3019–3024.
[17] Y. Abshirini, R. Foroutan, H. Esmaeili, Cr(VI) removal from aqueous solution using activated carbon prepared from *Ziziphus spina-christi* leaf, Mater. Res. Express, 6 (2019) 045607.
[18] I.S. Bădescu, D. Bulgariu, I. Ahmad, L. Bulgariu, Valorisation possibilities of exhausted biosorbents loaded with metal ions – a review, J. Environ. Manage., 24 (2018) 288–297.
[19] B.L. Zhao, J.-E. Zhang, W.B. Yan, X.W. Kang, C.G. Cheng, Y. Ouyang, Removal of cadmium from aqueous solution using waste shells of golden apple snail, Desal. Wat. Treat., 57 (2016) 23987–24003.
[20] R. Foroutan, A. Oujifard, F. Papari, H. Esmaeili, Calcined *Umbonium vestiarium* snail shell as an efficient adsorbent for treatment of wastewater containing Co(II), 3 Biotech., 9 (2019) 78.
[21] D. Alidoust, M. Kawahigashi, S. Yoshizawa, H. Sumida, M. Watanabe, Mechanism of cadmium biosorption from aqueous solutions using calcined oyster shells, J. Environ. Manage., 150 (2015) 103–110.
[22] Q. Wu, J. Chen, M. Clark, Y. Yu, Adsorption of copper to different biogentic oyster shell structures, Appl. Surf. Sci., 311 (2014) 264–272.
[23] K. Sbissi, V. Collière, M.L. Kahn, E.K. Hlil, M. Ellouze, F. Elhalouani, Fe doping effects on the structural, magnetic, and magnetocaloric properties of nano-sized $Pr_{0.6}Bi_{0.4}Mn_{1-x}Fe_xO_3$ ($0.1 \le x \le 0.3$) manganites, J. Nanostruct. Chem., 5 (2015) 313–323.
[24] S. Tamjidi, H. Esmaeili, Chemically modified CaO/Fe_3O_4 nanocomposite by Sodium dodecyl sulfate for Cr(III) removal from water, Chem. Eng. Technol., 42 (2019) 607–616.
[25] L.W. Fan, S.L. Zhang, X.H. Zhang, H. Zhou, Z.X. Lu, S.Q. Wang, Removal of arsenic from simulation wastewater using nano-iron/oyster shell composites, J. Environ. Manage., 156 (2015) 109–114.
[26] A.R.A. Usman, The relative adsorption selectivities of Pb, Cu, Zn, Cd and Ni by soils developed on shale in New Valley, Egypt, Geoderma, 144 (2008) 334–343.
[27] T.-C. Hsu, Experimental assessment of adsorption of Cu^{2+} and Ni^{2+} aqueous solution by oyster shell powder, J. Hazard. Mater., 171 (2009) 995–1000.
[28] M. Ahmadi, H. Rahmani, B. Ramavandi, B. Kakavandi, Removal of nitrate from aqueous solution using activated carbon modified with Fenton reagents, Desal. Wat. Treat., 76 (2017) 265–275.
[29] A. Günay, E. Arslankaya, I. Tosun, Lead removal from aqueous solution by natural and pretreated clinoptilolite: adsorption equilibrium and kinetics, J. Hazard. Mater., 146 (2007) 362–371.
[30] N. Ayawei, S.S. Angaye, D. Wankasi, E.D. Dikio, Synthesis, characterization and application of Mg/Al layered double hydroxide for the degradation of congo red in aqueous solution, Open J. Phys. Chem., 5 (2015) 56–70.
[31] H.K. Boparai, M. Joseph, D.M. O'Carroll, Kinetics and thermodynamics of cadmium ion removal by adsorption onto nano zerovalent iron particles, J. Hazard. Mater., 186 (2011) 458–465.
[32] M. Osińska, Removal of lead(II), copper(II), cobalt(II) and nickel(II) ions from aqueous solutions using carbon gels, J. Sol-Gel Sci. Technol., 81 (2017) 678–692.
[33] H. Ghassabzadeh, M. Torab-Mostaedi, A. Mohaddespour, M.G. Maragheh, S.J. Ahmadi, P. Zaheri, Characterizations of Co(II) and Pb(II) removal from aqueous solution using expanded perlite, Desalination, 261 (2010) 73–79.
[34] N.A. Negm, M.G.A. El Wahed, A.R.A. Hassan, M.T.H. Abou Kana, Feasibility of metal adsorption using brown algae and fungi: effect of biosorbents structure on adsorption isotherm and kinetics, J. Mol. Liq., 264 (2018) 292–305.
[35] S.Y. Huang, S. Song, R. Zhang, T. Wen, X.X. Wang, S.J. Yu, W.C. Song, T. Hayat, A. Alsaedi, X.K. Wang, Construction of layered double hydroxides/hollow carbon microsphere composites and its applications for mutual removal of Pb(II) and humic acid from aqueous solutions, ACS Sustainable Chem. Eng., 5 (2017) 11268–11279.
[36] Y. Du, J. Wang, Y.D. Zou, W. Yao, J. Hou, L.S. Xia, A. Peng, A. Alsaedi, T. Hayat, X.K. Wang, Synthesis of molybdenum disulfide/reduced graphene oxide composites for effective removal of Pb(II) from aqueous solutions, Sci. Bull., 62 (2017) 913–922.
[37] N. Wang, D.X. Yang, X.X. Wang, S.J. Yu, H.Q. Wang, T. Wen, G. Song, Z.M. Yu, X.K. Wang, Highly efficient Pb(II) and Cu(II) removal using hollow Fe_3O_4@PDA nanoparticles with excellent application capability and reusability, Inorg. Chem. Front., 5 (2018) 2174–2182.
[38] O. Yavuz, Y. Altunkaynak, F. Güzel, Removal of copper, nickel, cobalt and manganese from aqueous solution by kaolinite, Water Res., 37 (2003) 948–952.
[39] R. Foroutan, H. Esmaeili, M. Abbasi, M. Rezakazemi, M. Mesbah, Adsorption behavior of Cu(II) and Co(II) using chemically modified marine algae, Environ. Technol., 39 (2018) 2792–2800.
[40] X.X. Wang, Y. Liu, H.W. Pang, S.J. Yu, Y.J. Ai, X.Y. Ma, G. Song, T. Hayat, A. Alsaedi, X.K. Wang, Effect of graphene oxide surface modification on the elimination of Co(II) from aqueous solutions, Chem. Eng. J., 344 (2018) 380–390.
[41] S. Ben-Ali, I. Jaouali, S. Souissi-Najar, A. Ouederni, Characterization and adsorption capacity of raw pomegranate peel bioadsorbent for copper removal, J. Cleaner Prod., 142 (2017) 3809–3821.
[42] X. Xu, B.Y. Gao, Q.Y. Yue, Q. Li, Y. Wang, Nitrate adsorption by multiple biomaterial based resins: application of pilot-scale and lab-scale products, Chem. Eng. J., 234 (2013) 397–405.
[43] H. Esmaeili, R. Foroutan, Adsorptive behavior of methylene blue onto sawdust of sour lemon, date palm, and eucalyptus as agricultural wastes, J. Dispersion Sci. Technol., 40 (2019) 990–999.
[44] M. Arshadi, M.J. Amiri, S. Mousavi, Kinetic, equilibrium and thermodynamic investigations of Ni(II), Cd(II), Cu(II) and Co(II) adsorption on barley straw ash, Water Resour. Ind., 6 (2014) 1–17.
[45] Y.-H. Huang, C.-L. Hsueh, H.-P. Cheng, L.-C. Su, C.-Y. Chen, Thermodynamics and kinetics of adsorption of Cu(II) onto waste iron oxide, J. Hazard. Mater., 144 (2007) 406–411.
[46] M. Ahmadi, E. Kouhgardi, B. Ramavandi, Physico-chemical study of dew melon peel biochar for chromium attenuation from simulated and actual wastewaters, Korean J. Chem. Eng., 33 (2016) 2589–2601.